

# The Lithium Isotope Ratio in Metal-Poor Stars

P.E. NISSEN<sup>1</sup>, D.L. LAMBERT<sup>2</sup> and V.V. SMITH<sup>2</sup>

<sup>1</sup>*Institute of Physics and Astronomy, University of Aarhus, Denmark*

<sup>2</sup>*Department of Astronomy, University of Texas at Austin, U.S.A.*

## 1. Introduction

In the present article the scientific reasons for studying the lithium isotope ratio in stars are briefly reviewed, and the reduction and analysis of recent observations of the Li I 6707.8 Å resonance line in spectra of metal-poor stars are discussed in some detail. The aim and prospects of obtaining similar observations for fainter and more interesting stars with the ESO VLT are also touched upon.

## 2. Scientific Background

It is evident from the hundreds of astronomical papers of lithium published in the last 10 years that knowledge about the Li abundance in stars is of fundamental importance in studying the history of the Universe as well as the structure and evolution of stars. This is due to the many interesting processes by which lithium can be made at different times and places in the Universe. Most important is that Big Bang nucleosynthesis leads to a primordial abundance of Li, which depends on the physical conditions in the Big Bang phase, e.g. the baryon density and the degree of inhomogeneity. Measuring the primordial Li abundance therefore constrains Big Bang models. The discovery by Spite & Spite (1982) that the hotter Pop. II subdwarfs have a nearly constant Li abundance ( $\log \epsilon(\text{Li}) \approx 2.1$ , where  $\epsilon(\text{Li}) = N_{\text{Li}}/N_{\text{H}} \cdot 10^{12}$ ) suggests that this is the value of the primordial Li abundance in agreement with predictions from the Standard Big Bang model. Other processes may, however, have affected the Li abundance in the atmospheres of Pop. II stars. Li is produced by cosmic ray spallation of C, N, O nuclei and  $\alpha + \alpha$  fusion in the interstellar space. Possible stellar sources of Li include envelope burning in AGB stars and  $p + \alpha$  reactions in flares. In addition Li is destroyed by protons at the bottom of the convection zone if the temperature there is higher than about  $2 \times 10^6$  K. Hence, both Galactic and stellar evolution of lithium is a complicated affair, but by understanding the various processes better we will learn more about stellar and Galactic evolution and may be able to determine an accurate value of the primordial Li abundance.

In order to disentangle the relative importance of the various processes

that produce or destroy lithium it is important to know not only the total Li abundance but also the lithium isotope ratio  ${}^6\text{Li}/{}^7\text{Li}$ . The reason for this is that in some cases, e.g. Big Bang nucleosynthesis and envelope burning in AGB stars,  ${}^7\text{Li}$  only is produced, whereas other processes, e.g.  $\alpha + \alpha$  burning and flare events, produce both  ${}^6\text{Li}$  and  ${}^7\text{Li}$ . In addition,  ${}^6\text{Li}$  is destroyed more quickly than  ${}^7\text{Li}$  at the bottom of the convection zone in F and G stars.

The lithium isotope ratio in the solar system is known to be  ${}^6\text{Li}/{}^7\text{Li} = 0.08$  from analysis of meteorites. Recently, about the same ratio has been measured in the interstellar gas (Lemoine et al., 1993; Meyer et al. 1993). From earlier attempts to measure the isotope ratio in both Pop. I and II, F and G main sequence stars (Andersen et al. 1984, Maurice et al. 1984 and Pilachowski et al. 1989) an upper limit  ${}^6\text{Li}/{}^7\text{Li} < 0.10$  has been set. Recently,  ${}^6\text{Li}$  has, however, probably been detected in one Pop. II star (HD 84937,  $T_{\text{eff}} \approx 6200$  K and  $[\text{Fe}/\text{H}] \approx -2.4$ ) at a level of  ${}^6\text{Li}/{}^7\text{Li} = 0.05 \pm 0.02$  by Smith, Lambert & Nissen (1993). This abundance of  ${}^6\text{Li}$  in HD 84937 is about the value one would expect from the measured Be and B

abundances in metal-poor stars (Gilmore et al. 1991, Edvardsson et al. 1994) and the known cross sections for producing the isotopes of Li, Be and B by  $\alpha + \alpha$  fusion and C, N, O spallation, assuming a small degree of Li depletion as predicted by standard (non-rotating) stellar models. Models predicting a strong (factor of 10)  ${}^7\text{Li}$  depletion in subdwarfs seem to be excluded because according to these models there should be practically no  ${}^6\text{Li}$  left in HD 84937. Hence, the detection of  ${}^6\text{Li}$  supports the idea that the Li abundance in the hotter subdwarfs really represents the primordial abundance except for a small (10 %) contribution from Galactic cosmic ray processes.

In view of the important consequences of the detection of  ${}^6\text{Li}$  in HD 84937 independent determinations of the lithium isotope ratio in HD 84937 and other turnoff halo stars are very desirable. Furthermore, it would be interesting to study the  ${}^6\text{Li}/{}^7\text{Li}$  ratio as a function of  $[\text{Fe}/\text{H}]$  in order to see how the various processes mentioned above contribute to the evolution of Li in the Galaxy. In the following some new observations at ESO with this aim are described, and problems connected with

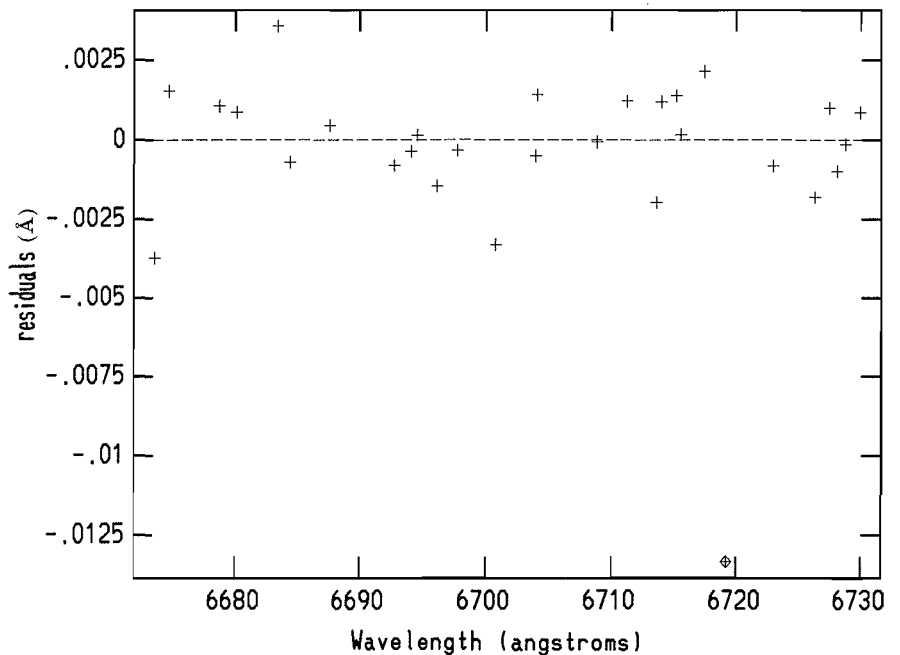


Figure 1: The residuals of the wavelength of 29 thorium lines from a 2nd-order dispersion solution. One strongly deviating line at 6719.2 Å is indicated by a special symbol. As discussed in the text this is caused by an argon line blending the thorium line. The rms deviation of the other lines is 1.5 mÅ.

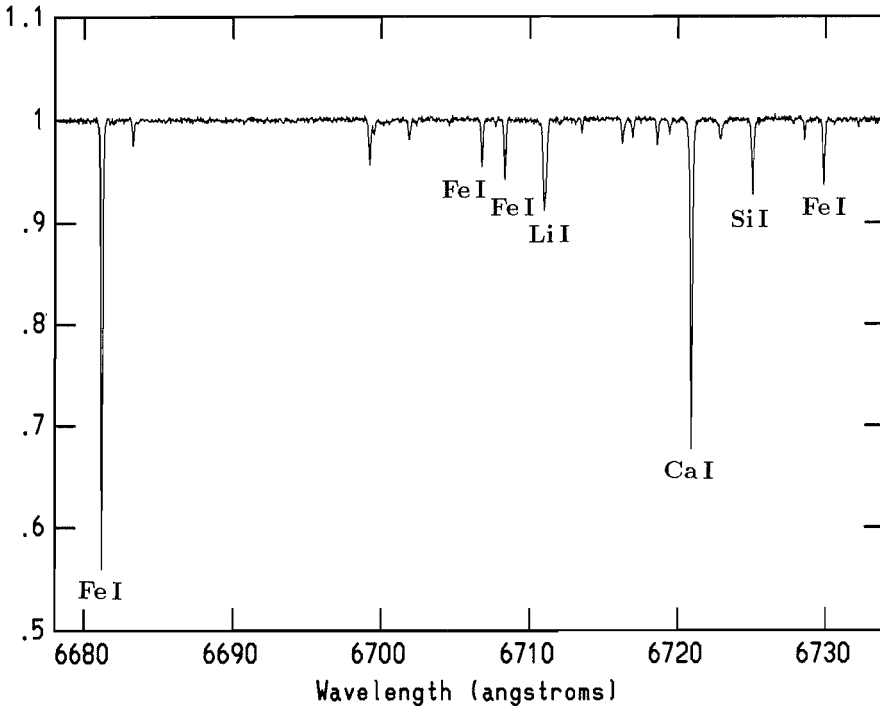


Figure 2: The spectrum of HD 76932 ( $V=5.8$ ) as observed with the ESO Coudé Echelle Spectrometer connected to the 3.6-m telescope by a fibre link. The lines used in connection with the determination of the lithium isotope ratio are identified. The spectrum has not been corrected for the Doppler shift due to the radial velocity of the star.

an accurate determination of the lithium isotope ratio are discussed.

### 3. Observations and Reductions

The spectral region around the Li I 6707.8 Å resonance line was observed with the ESO Coudé Echelle Spectrometer (CES) during 8 nights in October 1992 and 4 nights in June 1993. In October the 1.4-m CAT telescope was used, whereas the 3.6-m and the fibre link to the CES were used for the June observations. In both cases the long camera of the CES was applied providing a resolution of  $R=115,000$ . The corresponding entrance slit width of the CES for the CAT observations was 1.2 arcsec. In connection with the 3.6-m observations an image slicer was used so that the entrance aperture at the 3.6-m could be as large as  $3.4 \times 3.4$  arcsec. The detector was a  $2048 \times 2048$  FA chip with 15 micron pixels and a read-out noise of about  $10e^-$ .

The observing run with the CAT telescope was primarily used to observe a number of metal-poor ( $[Fe/H] \approx -0.8$ ) thick disk stars with magnitudes between 4 and 7, whereas the 3.6-m run was used for fainter halo stars with metallicities between  $-1.5$  and  $-2.1$ . The stars were selected to be in the turnoff region of Pop. II main sequence stars. Each star was observed on typically 4 different nights with slightly different settings of the central wavelength of the

CES to minimize the influence of possible defects of the CCD detector as well as irregularities in the flat-fielding procedure.

The spectra obtained were reduced with IRAF using tasks for subtraction of background, flat field correction, extraction of spectra, and wavelength calibration. Due to the use of an image slicer in connection with the 3.6-m observations each CCD frame consists of 8 individual spectra with different exposure levels. These were reduced separately and coadded after wavelength calibration. Finally, the spectra were rectified and normalized by fitting 5 pieces of cubic spline functions to the continuum.

Several aspects of the reductions are critical for the accuracy of the final spectra, in particular the wavelength calibration, the flat field correction and the determination of possible variations of the instrumental profile along the CCD caused by e.g. focus variations due to non-flatness of the CCD.

The wavelength calibration was performed by the aid of 29 thorium lines from a Th-Ar comparison lamp. A second order polynomial was adopted for the dispersion solution, i.e. wavelength vs. pixel coordinate. Residuals in the fit are shown in Figure 1. As seen the scatter is satisfactorily small, except for one strongly deviating line at 6719.2 Å. After contact with H. Hensberge, Brussels, who has made a detailed list of wavelengths of thorium lines including

notes on blends, it was cleared up that this deviating line is a close blend with an argon line. Excluding the 6719.2 Å line the rms deviation from the fit is 0.0015 Å or about 5% of the pixel width. We conclude that errors in the wavelength calibration are less than 0.002 Å or 2 mÅ. It should be noted that in the case of the 3.6-m observations the light from the Th-Ar lamp is sent via the fibre and through the image slicer. Hence, the light-pass through the optics of the CES is the same as for the star light. The same is true for the light from the flat fielding lamp. In the case of the CAT observations we don't have this favourable situation, so it is important that these observations are checked by observing some stars with both systems.

Figure 2 shows the combined spectrum of HD 76932 ( $T_{\text{eff}} = 5970$  K,  $[Fe/H] = -0.8$ ) obtained on June 6 and 8, 1993 with the fibre link to the 3.6-m telescope. The S/N of the spectrum is about 600. Figure 3 shows a detail of the region around the Li I line. For comparison the spectrum of HR 7121, an early B-type star with no spectral lines in this region, is also shown. It was reduced in the same way as HD 76932. As seen the spectrum of HR 7121 is indeed flat within its S/N of about 800.

Figure 3 also shows the profile of an unblended thorium line. It is symmetric and is well fitted by a Gaussian profile with a FWHM = 58 mÅ corresponding to a resolution of  $R=115,000$ . It was checked that there is no significant variation of this profile along the CCD; the FWHM varies between 58 and 60 mÅ only. Hence, we can assume that there are no focus variations along the spectrum, which is important when applying the profile method to determine the lithium isotope ratio.

In Figure 3 it is not possible to see the very broad, low-intensity wings that are always present in the profile of a spectrometer. The effect of these wings is equivalent to stray light in the dispersion direction, which one cannot account for by subtracting the light scattered perpendicular to the dispersion direction. From measurements of the profile of the laser line at 6328 Å it is, however, known that the equivalent amount of stray light for the CES in the red part of the spectrum is 1–2% only. Hence, it has only a marginal effect on the profiles of weak lines, but may in any case be included in the reductions.

### 4. Analysis

The Li I resonance line is a doublet with hyperfine structure. Accurate interferometric wavelength measurements have been carried out by Meissner et al.

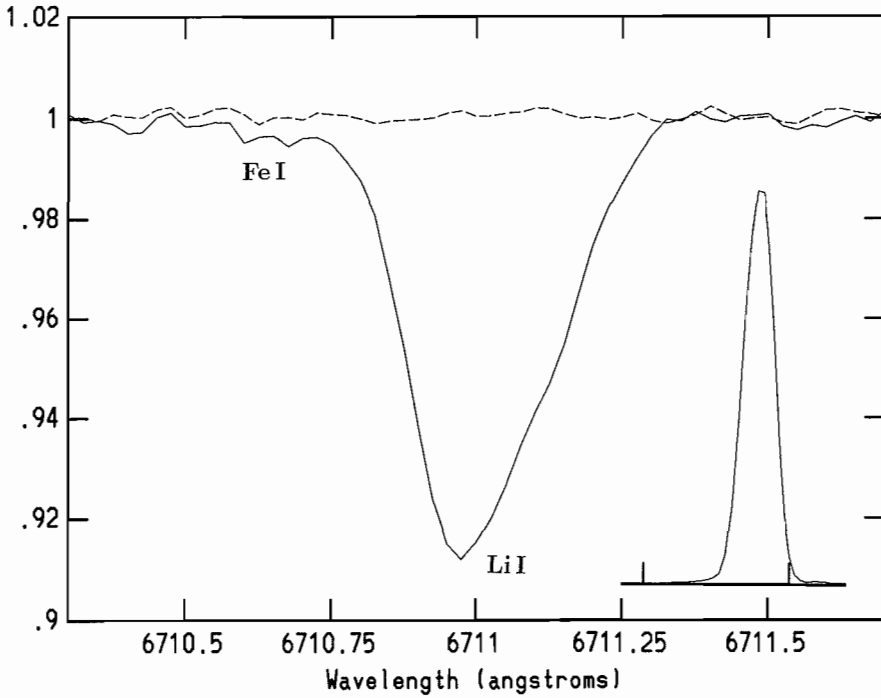


Figure 3: Detail of Figure 2. In addition to the Li I line a weak blending Fe I line is seen. For comparison the spectrum of an early B-type star, HR 7121 ( $V = 2.1$ ) having no spectral lines in this region is shown with a dashed line. Furthermore, a thorium line is inserted in order to illustrate the instrumental profile of the CES.

(1948). The doublet splitting is  $0.152 \text{ \AA}$  and the isotope shift is  $0.158 \text{ \AA}$  with  ${}^6\text{Li}$  having the longest wavelength (see Table 1 of Andersen et al. 1984). Hence, the stronger doublet component of  ${}^6\text{Li}$  is superimposed on the weaker  ${}^7\text{Li}$  component. Due to the various line broadening effects in a stellar atmosphere a rather complicated profile results. Figure 5 shows a model-atmosphere calculation of the Li line in HD 76932 for three values of  ${}^6\text{Li}/\text{Li}$ . As seen an increase of the  ${}^6\text{Li}$  abundance has two effects: (i) a shift of the centre-of-gravity wavelength of the Li line amounting to  $15 \text{ m\AA}$  when  ${}^6\text{Li}/\text{Li}$  is increased from 0.0 to 0.1, and (ii) an increase of the FWHM of the line, which amounts to  $18 \text{ m\AA}$  for the same increase of  ${}^6\text{Li}/\text{Li}$ . It means, that we have essentially two methods to determine the  ${}^6\text{Li}/{}^7\text{Li}$  ratio: The centre-of-gravity method and the profile method. In the following we discuss these methods separately.

#### 4.1 ${}^6\text{Li}/{}^7\text{Li}$ from centre-of-gravity (cog) wavelengths

When measuring the cog-wavelength of the Li line we must reduce the observed wavelength for the Doppler shift due to the radial velocity of the star and the gravitational redshift. In the case of HD 76932 the Doppler shift was determined from the lines identified in Figure 2. In metal-poor stars these lines are practically unblended. Very accurate wavelengths of the Fe I lines have recently been published by Nave et al. (1994). Furthermore, M. Rosberg and S. Johansson, Lund, have kindly measured a similar accurate wavelength of the Ca I line. The error of these wavelengths (Table 1) is less than  $2 \text{ m\AA}$ . The wavelength of the Si I line was adopted from Kurucz & Peytreman (1975) and is less accurate.

How well do the Doppler shifts determined from the various lines agree?

Table 2. The difference  $\Delta\lambda$  between the measured cog-wavelength of the Li I line and the cog-wavelength corresponding to  ${}^6\text{Li}/{}^7\text{Li} = 0.0$ . The last column gives the equivalent width of the Li line.

Night	$\Delta\lambda$	W(Li)
Oct. 24, 1992	$6.8 \text{ m\AA}$	$24.9 \text{ m\AA}$
Oct. 25, 1992	$6.2$	$24.4$
Oct. 26, 1992	$8.8$	$23.5$
June 6, 1993	$3.7$	$24.5$
June 8, 1993	$4.7$	$26.0$
Average	$6.0 \text{ m\AA}$	$24.7 \text{ m\AA}$

Table 1 shows for each night the difference between the Doppler shift (in  $\text{km s}^{-1}$ ) determined from an individual line and the mean Doppler shift for the six lines. As seen, there are some systematic differences which repeat from night to night. The weak, high-excitation lines appear to be slightly blueshifted (about  $0.2 \text{ km s}^{-1}$  or  $4 \text{ m\AA}$ ) relative to the stronger, lower excitation potential lines (Fe I at  $6678.0 \text{ \AA}$  and Ca I at  $6717.7 \text{ \AA}$ ). It may be due to small errors in the laboratory wavelengths, but it could also be caused by convective motions. In fact, similar systematic differences are seen in the solar spectrum (Dravins et al. 1981), and have been explained by a hydrodynamical model in which hot, rising bright granules are balanced by a downflow in darker (cooler) inter-granular regions. The result is a convective blueshift of the lines, which is more pronounced for the weak high-excitation lines because they are formed deep in the atmosphere where the convective motions are more vigorous.

Assuming that the convective blueshift of the Li I resonance line is the same as the mean shift of the Fe I  $6678.0 \text{ \AA}$  and Ca I  $6717.7 \text{ \AA}$  lines, the observed cog-wavelengths have been corrected for Doppler shift. The resulting difference,  $\Delta\lambda$ , relative to the cog-wavelength corresponding to  ${}^6\text{Li}/{}^7\text{Li} = 0.0$  ( $6707.812 \text{ \AA}$ ) is listed in Table 2. As seen, the results from the various nights agree quite well. The average value of  $\Delta\lambda$  is  $6.0 \text{ m\AA}$ , which would correspond to  ${}^6\text{Li}/{}^7\text{Li} = 0.04$  if the shift was due to

Table 1: Values of  $\Delta V = V_{\text{indv.}} - V_{\text{mean}}$  for HD 76932 as observed on 5 different nights.  $V_{\text{indv.}}$  is the Doppler shift in  $\text{km s}^{-1}$  determined from a single line and  $V_{\text{mean}}$  is the mean Doppler shift for all six lines. The first 3 nights are from the Oct. 1992 observing run with the CAT, and nights 4 and 5 are from the June 1993 run with the fibre link to the 3.6 m. In col. 2 the excitation potential of the lower level of the line is given. Col. 3 lists the laboratory wavelength taken from sources given in the text and col. 4 the measured equivalent width of the line.

Line	$\chi$	$\lambda_{\text{lab}}$	W	$\Delta V_1$	$\Delta V_2$	$\Delta V_3$	$\Delta V_4$	$\Delta V_5$	$\Delta V_{\text{mean}}$
Fe I	2.69 eV	$6677.987 \text{ \AA}$	$73 \text{ m\AA}$	0.14	0.15	0.10	0.25	0.13	0.15
Fe I	2.76	$6703.567$	6	0.27	0.05	-0.04	-0.07	0.04	0.04
Fe I	4.61	$6705.102$	9	-0.24	-0.10	0.07	-0.15	-0.04	-0.09
Ca I	2.71	$6717.677$	61	0.21	0.25	0.25	0.25	0.23	0.24
Si I	5.86	$6721.848$	13	-0.34	-0.34	-0.48	-0.28	-0.39	-0.37
Fe I	4.61	$6726.667$	10	0.05	-0.01	0.12	0.02	0.04	0.04

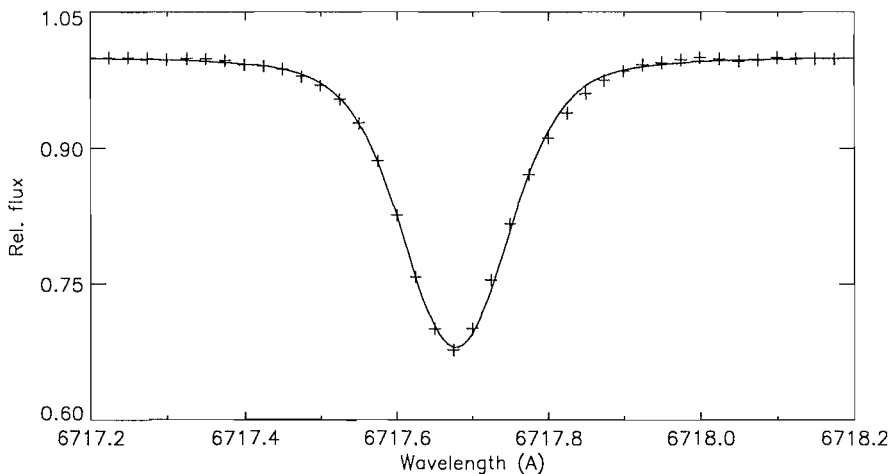


Figure 4: The observed profile of the CaI line of HD 76932 (+) compared with a synthetic model atmosphere profile convolved with a radial-tangential broadening function with the FWHM = 4.7 km s<sup>-1</sup>. A slight asymmetry in the right wing of the observed profile is evident. It corresponds to a C-shaped line bisector.

the presence of <sup>6</sup>Li. Differential convective blueshifts between the LiI line and the comparison lines may, however, be responsible for the positive value of  $\Delta\lambda$ . It is therefore doubtful that <sup>6</sup>Li has been detected in HD 76932.

The total Li abundance of HD 76932 derived from the equivalent width ( $W = 24.7$  mÅ) of the LiI line is  $\epsilon(\text{Li}) = 2.06$ , close to the value at the “Spite” plateau for halo stars. Two other stars observed (HD 22879 and HD 63077), have a much weaker Li line ( $W = 7$  mÅ) despite the fact that they have about the same  $T_{\text{eff}}$  and  $[\text{Fe}/\text{H}]$  as HD 76932. Their atmospheres are depleted in Li by a factor of 4–5, and we would therefore expect that they are totally depleted in <sup>6</sup>Li. Still, the apparent <sup>6</sup>Li/<sup>7</sup>Li ratio derived from the cog-wavelength is about 0.04. This points to a zero-point error in the method, probably due to differential convective blueshifts between the Li line and the FeI and CaI lines used for determining the Doppler shift of the star. We conclude that <sup>6</sup>Li has not been detected in HD 76932. The upper limit for <sup>6</sup>Li/<sup>7</sup>Li is about 0.03.

#### 4.2. <sup>6</sup>Li/<sup>7</sup>Li from the profile of the LiI line

As an example of this method we again use the spectrum of HD 76932. Synthetic spectra have been computed by the aid of a programme BSYN kindly made available by the stellar atmosphere group in Uppsala. The model atmosphere used has parameters,  $T_{\text{eff}} = 5970$  K,  $\log g = 4.4$  and  $[\text{Fe}/\text{H}] = -0.8$ . Details about the construction of the model and the determination of the model parameters of HD 76932 are given by Edvardsson et al. (1993). The model atmosphere computation in-

cludes thermal and microturbulent broadening with  $\xi_{\text{turb}} = 1.4$  km s<sup>-1</sup> as determined by Edvardsson et al. In addition, the profiles of the lines are broadened by macroturbulent motions, rotation of the star and the instrumental profile. The synthetic spectrum was therefore folded by various broadening functions in order to reproduce the observed profiles of the FeI and CaI lines. It turns out that neither an isotropic Gaussian function nor a pure rotation profile lead to a satisfactory agreement between the observed and the synthetic profile. The best fit is obtained with a so-called radial-tangential profile (Gray 1976), which corresponds to radial and tangential motions in the atmosphere each with a Gaussian distribution of the velocities. The radial-tangential profile is more V-shaped than the U-shaped profiles corresponding to pure rotation or isotropic Gaussian broadening.

Figure 4 shows the resulting fit for the CaI line at 6717.7 Å. The equivalent width is the same for the observed and the synthetic line. A FWHM = 4.7 km s<sup>-1</sup> of the radial-tangential convolution profile is required to get the best overall fit. As seen, the fit is, however, not perfect. A slight asymmetry is apparent in the right wing of the Ca line. The observed points in the lower part of the line fall to the left of the synthetic line, whereas the points in the upper part fall to the right. Similar deviations are seen for the FeI lines in the spectrum of HD 76932. The asymmetry corresponds to a C-shaped line bisector, defined as the loci of points midway between equal-intensity points on either side of a line. C-shaped bisectors are well known for solar lines (Dravins et al. 1981) and have also been measured for a few of the brightest solar-type stars (Dravins 1987). Again, they

can be explained by convective motions. The brighter rising granules form a blueshifted component of the line, whereas the darker sinking regions form a weaker redshifted component. Although the effect on the line profile is small it has to be taken into account when one wants to determine very accurate values of the <sup>6</sup>Li/<sup>7</sup>Li ratio.

Figure 5 shows the observed profile of the LiI line of HD 76932 compared to three synthetic profiles corresponding to <sup>6</sup>Li/Li = 0.0, 0.1 and 0.2. The radial-tangential broadening function determined from the analysis of the CaI line has been applied. As seen, the profile corresponding to <sup>6</sup>Li/<sup>7</sup>Li = 0.0 gives a nearly perfect fit to the data, especially when one takes into account the small asymmetry inherent in the observed CaI profile. Hence, like in the case of the cog-wavelength method there is no evidence of the presence of <sup>6</sup>Li. From Figure 5 an upper limit <sup>6</sup>Li/<sup>7</sup>Li < 0.03 can be set.

## 5. Results and the Need for VLT Observations

The spectrum of HD 76932 has been discussed in some detail above to illustrate the methods and accuracies by which the <sup>6</sup>Li abundance in metal-poor stars can be determined. Results for other stars observed at ESO will be published in another paper. Here it should just be mentioned that for most of the stars studied <sup>6</sup>Li seems not to be present in the atmosphere. This may well be due to the fact that these stars are too cool ( $T_{\text{eff}} < 6000$  K) for <sup>6</sup>Li to survive depletion at the bottom of the convection zone. Somewhat hotter stars at the very bluest point of the Pop. II turnoff sequence, like HD 84937 ( $T_{\text{eff}} \approx 6200$  K) are more interesting candidates for <sup>6</sup>Li determinations. But these stars are rare. One such star (CD -30°18140,  $[\text{Fe}/\text{H}] = -2.1$ ) was observed with the fibre link to the 3.6-m. However, due to its faintness ( $V = 10.0$ ), the S/N obtained is not quite sufficient for an accurate determination of the <sup>6</sup>Li/<sup>7</sup>Li ratio despite the fact that a total of 10 hours of observing time was spent on the star.

There is a clear need for the light collecting power of the ESO VLT to reach a statistically significant sample of metal-poor stars at the turnoff point. With the planned UVES instrument it will be possible to reach  $R = 120,000$  in the red, which is sufficient for determinations of the <sup>6</sup>Li/<sup>7</sup>Li ratio. However, because of the use of an R4 echelle grating in UVES, the tilt of spectral lines along one order will change quite significantly ( $\pm 1.4^\circ$ ), and the dispersion will change by about 30%. This puts high demands on the reduction software if high S/N

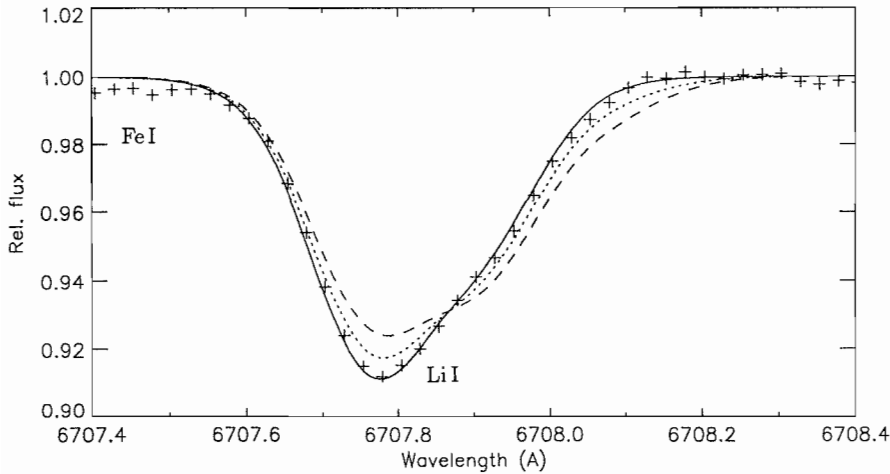


Figure 5: The observed profile of the Li I line of HD 76932 (+) compared with synthetic model atmosphere profiles convolved with a radial-tangential broadening function with the FWHM =  $4.7 \text{ km s}^{-1}$  and corresponding to  ${}^6\text{Li}/\text{Li} = 0.0, 0.1$  and  $0.2$ , respectively. The position of a weak Fe I line at  $6707.4 \text{ \AA}$  is marked.

(> 400) and accurate wavelength calibration are to be obtained. A dedicated spectrometer with a well-defined profile similar to the CES but allowing resolutions up to  $R = 300,000$  for a limited spectral region, say  $\Delta\lambda = 100 \text{ \AA}$ , would be a better instrument for a  ${}^6\text{Li}$  programme. In addition, such an instrument

would be needed for many other programmes like studies of the hydrodynamics of stellar atmospheres and the composition of interstellar gas.

#### References

Andersen, J., Gustafsson, B., Lambert, D.L. 1984, *A&A* **136**, 65.

Dravins, D. 1987, *A&A* **172**, 211.  
 Dravins, D., Lindegren, L., Nordlund, Å. 1981, *A&A* **96**, 345.  
 Edvardsson, B., Andersen, J., Gustafsson, B., Lambert, D.L., Nissen, P.E., Tomkin, J. 1993, *A&A* **275**, 101.  
 Edvardsson, B., Gustafsson, B., Johansson, S.G., Kismann, D., Lambert, D.L., Nissen, P.E., Gilmore, G. 1994, *A&A* (in press).  
 Gilmore, G., Gustafsson, B., Edvardsson, B., Nissen, P.E. 1992, *Nature* **357**, 379.  
 Gray, D.F. 1976, "The Observation and Analysis of Stellar Photospheres", John Wiley and Sons, p. 426.  
 Kurucz, R.L. Peytremann, E. 1975, *Smithsonian Astrophys. Obs. Spec. Rep.* 362.  
 Lemoine, M., Ferlet, R., Vidal-Madjar, A., Emerich, C., Bertin, P. 1993, *A&A* **269**, 469.  
 Maurice, E., Spite, F., Spite, M. 1984, *A&A* **132**, 278.  
 Meissner, K.W., Mundie, L.G., Stelson, P.H. 1948, *Phys. Rev.* **74**, 932.  
 Meyer, D.M., Hawkins, I., Wright, E.L. 1993, *ApJ* **409**, L61.  
 Nave, G., Johansson, S., Learner, R.C.M., Thorne, A.P., Brault, J.W. 1994, *ApJS* (in press).  
 Pilachowski, C.A., Hobbs, L.M., De Young, D.S. 1989, *ApJ* **345**, L39.  
 Smith, V.V., Lambert, D.L., Nissen, P.E. 1993, *ApJ* **408**, 262.  
 Spite, F., Spite, M. 1982, *A&A* **115**, 357.

## The Kinematics of the Planetary Nebulae in the Outer Regions of NGC 1399

M. ARNABOLDI<sup>1</sup>, K.C. FREEMAN<sup>1</sup>, X. HUI<sup>2</sup>, M. CAPACCIOLI<sup>3,4</sup> and H. FORD<sup>5</sup>

<sup>1</sup>Mt. Stromlo Observatory, Canberra ACT, Australia

<sup>2</sup>Astronomy Department, California Institute of Technology, Pasadena, U.S.A.

<sup>3</sup>Dipartimento di Astronomia, Università di Padova, Padova, Italy

<sup>4</sup>Osservatorio Astronomico di Capodimonte, Napoli, Italy

<sup>5</sup>Physics and Astronomy Department, The Johns Hopkins University, Baltimore, U.S.A.

### 1. Introduction

Integrated light observations of the inner regions of giant elliptical galaxies indicate that most of them are slow rotators (e.g. Capaccioli & Longo 1994), with specific angular momentum  $J/M$  that is 5 to 10 times less than for the disks of giant spirals (e.g. Fall 1983). Cosmological simulations (e.g. Zurek et al. 1988) show that  $J/M$  should be similar in a cluster environment (where spheroidal systems are preferentially found) and in the field (where the disk galaxies predominate). As a way around this problem, Hui et al. (1993) suggested that much of the angular momentum of these elliptical galaxies may reside in their outermost parts (beyond 20 kpc), which cannot be studied by integrated

light techniques. This suggestion was made following the recent radial velocity measurements of 500 planetary nebulae (PN) in the giant elliptical Centaurus A, extending out to about 20 kpc from the nucleus (for comparison, kinematical observations from integrated light reach out only about 5 kpc from the nucleus). The velocities of the PNe in Cen A showed a surprising result: its outer halo is rapidly rotating. The mean rotational velocity rises slowly from the centre of the galaxy and flattens to a value of about 100 km/s between 10 and 20 kpc from the centre. This property was not at all apparent from the integrated light observations of the inner regions. Another very interesting dynamical feature of Cen A is that its metal-weak

globular cluster system, which also extends out to about 20 kpc, does not appear to be rotating at all (Harris et al. 1988).

Cen A is an unusual and disturbed elliptical system. One would like to investigate the outer halo of undisturbed ellipticals to see (i) if their old stellar populations are also rapidly rotating and (ii) if their globular cluster systems are non-rotating, as in Cen A. It would be interesting to make such a study for normal giant ellipticals and also for the dominant giant ellipticals in clusters. Many of these cD galaxies have huge globular cluster populations and extended halos, and may well have different formation histories. The nearest of these giant galaxies, at distances of